Structural transitions of ordered kesterite-type Cu_2ZnSnS_4 under pressure

I. Efthimiopoulos, A. Ritscher, M. Lerch, S. Speziale, A. S. Pakhomova, H. P. Liermann, and M. Koch-Müller

Citation: Appl. Phys. Lett. **110**, 041905 (2017); doi: 10.1063/1.4974941
View online: http://dx.doi.org/10.1063/1.4974941
View Table of Contents: http://aip.scitation.org/toc/apl/110/4
Published by the American Institute of Physics

Structural transitions of ordered kesterite-type Cu_2ZnSnS_4 under pressure

I. Efthimiopoulos,[1,a)] A. Ritscher,[2,3] M. Lerch,[2] S. Speziale,[1] A. S. Pakhomova,[4] H. P. Liermann,[4] and M. Koch-Müller[1]
[1]*Deutsches GeoForschungsZentrum GFZ, Section 4.3, Telegrafenberg, 14473 Potsdam, Germany*
[2]*Institut für Chemie, Technische Universität Berlin, Strasse des 17 Juni 135, 10623 Berlin, Germany*
[3]*Helmholtz-Zentrum Berlin für Materialien und Energie, Hahn-Meitner-Platz 1, 14109 Berlin, Germany*
[4]*Deutsches Elektronen-Synchrotron DESY, Notkestrasse 85, D-22603 Hamburg, Germany*

(Received 21 October 2016; accepted 13 January 2017; published online 25 January 2017)

We have investigated the high-pressure structural and vibrational behavior of the ordered kesterite-type Cu_2ZnSnS_4 compound. Our investigations have revealed two structural transitions: a kesterite-to-disordered kesterite transition was observed between 7 and 9 GPa, which involves a Zn/Cu disorder within the respective cationic sublattice, whereas a rocksalt-type structure was realized at ~15 GPa. The latter transition is accompanied by a cationic coordination increase from fourfold-to-sixfold with respect to the sulfur anions. The predicted kesterite-to-stannite transition was not detected. Furthermore, our high-pressure Raman studies have shown that the aforementioned Zn/Cu cationic disorder will *always* be present in Cu_2ZnSnS_4 under relatively moderate compression. *Published by AIP Publishing.* [http://dx.doi.org/10.1063/1.4974941]

The quaternary semiconductor Cu_2ZnSnS_4 has attracted considerable attention in recent years due to its potential utilization in photovoltaic devices.[1,2] The suitability of this material for solar cell applications stems from its almost optimal band gap ($E_g \sim 1.5$ eV), its high absorption coefficient in the visible range ($\sim 10^4$ cm^{-1}), and its earth-abundant, low-cost, and non-toxic constituents.[3–5] The current record of the Cu_2ZnSnS_4 thin films' power conversion efficiency is ~9%,[6] still far away from the theoretical limit of ~30%.[7] Hence, it becomes imperative to explore the physical properties of this material further, as a means of improving its photovoltaic performance.

At ambient conditions, Cu_2ZnSnS_4 crystallizes in the kesterite (KS) structure (SG $I\bar{4}$, $Z = 2$, Fig. 1).[8,9] This phase is structurally derived from the sphalerite-type structure by a doubling of the respective c-axis, resulting from alternating cationic (Cu/Sn or Cu/Zn) layers separated by sulfur anions.[10] Consequently, all of the cations are tetrahedrally coordinated with respect to the anions. Even though the KS phase represents an ordered cationic arrangement, i.e., each cation occupies a unique Wyckoff site, cationic disorder is quite common in this material.[8,11–14] Such a disorder can affect the photovoltaic properties of this system. For example, a mixed occupancy between Cu and Zn in the $z = 1/4$ and $z = 3/4$ cationic layers results in a disordered kesterite configuration (DKS, SG $I\bar{4}\,2m$, $Z = 2$, Fig. 1) and a subsequent reduction of E_g.[5,15]

The layered arrangement of the KS structure implies the anisotropic susceptibility of its physical properties to strain. Indeed, two separate theoretical works have investigated the effect of strain on the electronic properties of Cu_2ZnSnS_4.[16,17] In particular, an application of compressive strain is found to increase E_g, whereas a KS-to-stannite[18] (ST) structural transition was predicted at about 32 GPa.[17] Partly motivated by the aforementioned studies, and given that there are no experimental high-pressure studies on this system to date, we have investigated the pressure-induced structural and vibrational behavior of the ordered Cu_2ZnSnS_4 compound by means of X-ray diffraction (XRD) and Raman spectroscopy. The latter is a well-established method for detecting the various types of structural disorder in this material.[14,19–22] Even though we have not detected the proposed KS-to-ST transition, we have clearly identified a KS-to-DKS transition between 7 and 9 GPa, whereas another rocksalt-type (RS) structure was observed at about 15 GPa.

Details of the Cu_2ZnSnS_4 powder sample synthesis can be found in Ref. 23. Pressure was generated with a symmetric diamond anvil cell (DAC) with 400 μm culet diamonds. Drilled pre-indented steel or rhenium gaskets with hole diameters of 150–200 μm served as sample chambers in separate runs. The ruby luminescence method was used for measuring pressure.[24] Angle-resolved high-pressure powder XRD measurements were performed at the Extreme Conditions Beamline P02.2 of PETRA III (Hamburg, Germany)[25] with an incident X-ray wavelength $\lambda = 0.289$ Å and a beam size of 2 μm × 2 μm. Two-dimensional XRD patterns were collected with a fast flat panel detector XRD1621 from PerkinElmer (2048 pixels × 2048 pixels, 200 × 200 μm^2 pixel size) and processed with the FIT2D software.[26] Refinements were performed using the

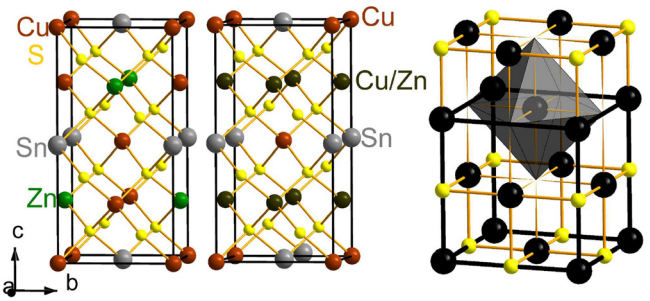

FIG. 1. Unit cell of kesterite (KS, SG $I\bar{4}$, $Z = 2$, left), disordered-KS (SG $I\bar{4}\,2m$, $Z = 2$, middle), and the high-pressure NaCl-type phase (RS, SG $Fm\bar{3}m$, $Z = 4$, right) phases. The brown, green, gray, and yellow spheres represent Cu, Zn, Sn, and S ions, respectively.

a)Author to whom correspondence should be addressed. Electronic mail: ilias.efthymiopoulos@gfz-potsdam.de

GSAS+EXPGUI software packages.[27] The high-pressure Raman measurements were conducted with a Horiba Jobin Yvon LabRam HR800 VIS spectrometer, equipped with a blue ($\lambda = 473$ nm) diode-pumped solid-state laser. The incident laser power was kept sufficiently low, in order to avoid any heating-induced order-disorder transition.[22,28] Argon served as a pressure transmitting medium (PTM) in all high-pressure experiments. We note that Ar becomes solid at 1.4 GPa,[29] whereas we used its equation of state (EoS) for additional pressure calibration.[30,31] In order to ensure the quasi-hydrostatic conditions, we followed the instruction of Wittlinger *et al.*[32] and annealed the DAC at 8 GPa to 120 °C for 30 min.[33]

In Figs. 2(a) and 2(b), we summarize our high-pressure Raman spectroscopic results on Cu_2ZnSnS_4. For the KS phase, we expect a sum of 15 Raman-active modes[34]

$$\Gamma = 3A + 6B + 6E. \quad (1)$$

At ambient conditions, we could resolve 12 Raman modes (Table S1 in supplementary material). We note that only 4–5 Raman-active modes are clearly visualized in our Raman spectra (Fig. 2); the remaining Raman features arise from the careful inspection of the low-intensity part of the measured spectra (Figs. 2 and S2 in supplementary material). The ambient-pressure Cu_2ZnSnS_4 Raman response is consistent with the reported Raman spectra collected either with green or blue laser light excitation,[14,19,34,35] with the strongest KS Raman features lying at 291 cm^{-1} and 338 cm^{-1} (sulfur-related vibrations).[34] Upon applying relatively moderate pressure, we noticed a change in the Raman spectrum of Cu_2ZnSnS_4 [Fig. 2(a)]. In particular, we observed the development of a broad sideband at 335 cm^{-1} [denoted as "D" in Fig. 2(a)]; this effect was reproducible in separate runs. Even though this D-band has been attributed to the disordered KS modification,[14,15,22,34] a phonon confinement effect has been also suggested behind its origin.[36] Since our sample is bulk polycrystalline powder and not a thin film, and considering that the as-synthesized DKS powder sample shows its most intense band at ~335 cm^{-1} (supplementary material), we attribute this D-band to the existence of a partially disordered kesterite arrangement under moderate compression. This observation seems quite plausible, if we take into account the low formation energy of this particular type of cationic disorder.[11,12]

In Fig. 2(b), we plot the Raman spectra of Cu_2ZnSnS_4 at selected pressures. The respective Raman mode frequencies' evolution as a function of pressure is provided in Fig. S1 in the supplementary material. Upon increasing pressure, all the Raman-active modes shift to higher frequencies as expected. In addition, the D-band becomes more enhanced upon compression, at the expense of the KS-related 338 cm^{-1} mode. Following Ref. 14, and by assuming that both KS and DKS phases have similar Raman cross-sections, we estimated the degree of disorder by the area peak ratio of the 338 cm^{-1} (KS) to the 335 cm^{-1} mode (DKS) [inset of Fig. 2(a)]. Our results indicate that the DKS modification becomes the dominant phase at about 9 GPa.

Increasing pressure further results in another change of the Cu_2ZnSnS_4 Raman response close to 15 GPa, with the vanishing of the KS/DKS-related Raman features and the appearance of a broad band at ~350 cm^{-1}. We interpret this Raman-related change as a second transition of Cu_2ZnSnS_4. Upon decompression, we recover a Raman signal reminiscent of the original phase, yet with a substantial disorder as indicated by the broad Raman features. We tentatively term this recovered phase as DKS-II, as it appears to correspond to a different disordered Cu_2ZnSnS_4 modification. Interestingly, similar metastable disordered modifications have been observed for several defect chalcopyrites upon decompression.[37–39] The structural identification of this DKS-II phase is left for future experiments.

Following our Raman results, we have performed the *in situ* high-pressure XRD investigations on Cu_2ZnSnS_4 in order to identify the structural changes under compression.

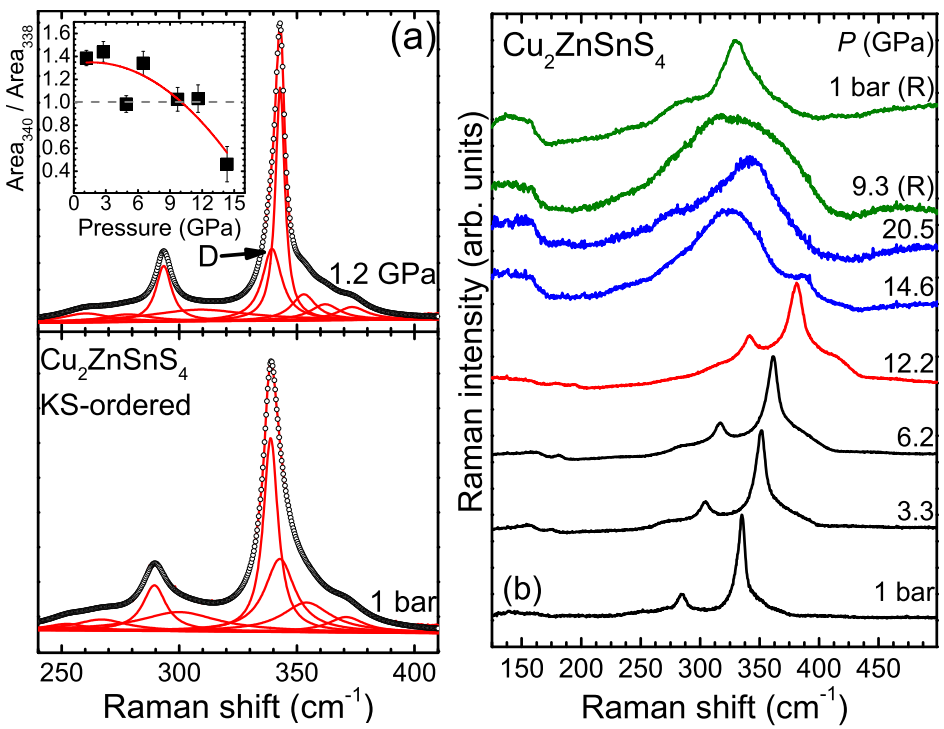

FIG. 2. (a) Deconvolution of the Cu_2ZnSnS_4 Raman spectra with Lorentzian functions at ambient pressure and at 1.2 GPa. The D band denotes the strongest disordered-kesterite feature. Inset: Raman peak area ratio of the 338 cm^{-1} (KS) and the 335 cm^{-1} (DKS) bands as a function of pressure (note that these are the ambient-pressure frequency values for the two modes). The red solid line is a guide for the eye. (b) Raman spectra of Cu_2ZnSnS_4 at selected pressures. The black, red, blue, and green spectra correspond to the KS, DKS, RS, and DKS-II phases, respectively.

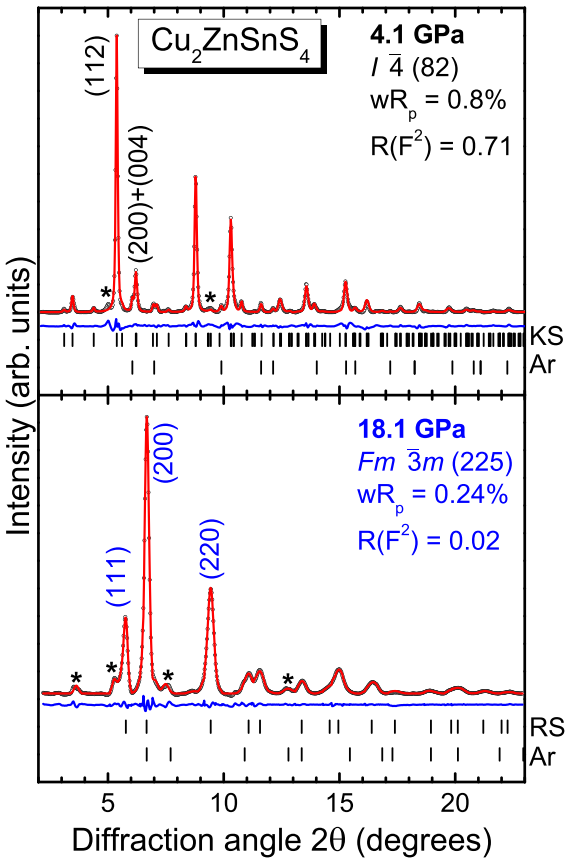

FIG. 3. Refined XRD patterns for the KS (4.1 GPa, top) and the RS-type (18.1 GPa, bottom) phases of Cu_2ZnSnS_4. Dots correspond to the measured spectra and the red solid lines represent the best Rietveld refinements. The difference spectra between the measured and the refined patterns are depicted too (blue curves). Vertical ticks mark the Bragg peak positions. Asterisks mark the strongest Bragg peaks of the Cu_2S impurity phase.

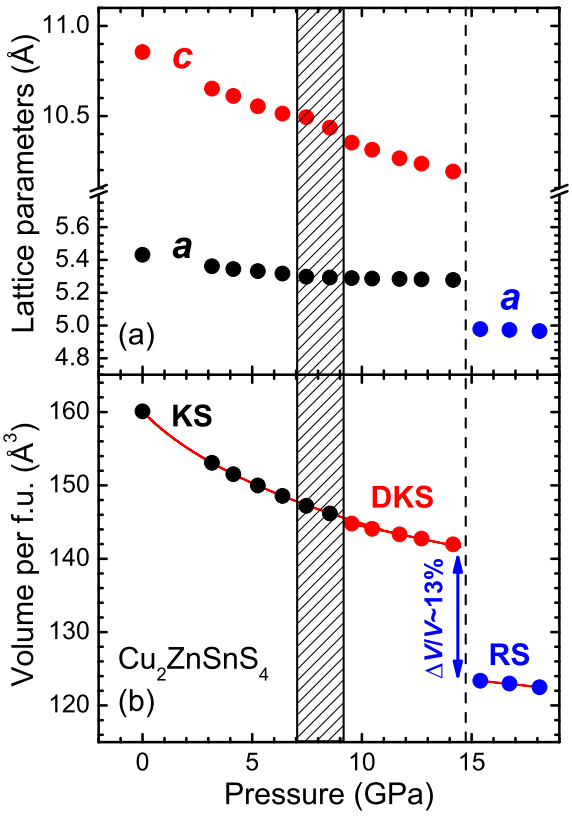

FIG. 4. (a) Lattice constants and (b) unit cell volume per formula unit as a function of pressure for the various phases of Cu_2ZnSnS_4. Error bars lie within the symbols. The shaded area and the vertical dashed line mark the range and the onset pressure of the KS-to-DKS and DKS-to-RS structural transitions, respectively. The solid lines represent the fitted Birch-Murnaghan EoS functions.

Generally, the quality of the obtained XRD patterns allowed us to perform full Rietveld refinements (Fig. 3). Here, however, we focus only on the pressure-induced behavior of the lattice parameters (Fig. 4); a more extensive discussion and comparison with relevant compounds (e.g., in Refs. 40 and 41) will be provided elsewhere. We should state that minor traces of Cu_2S were detected at ambient conditions (Fig. S3 in supplementary material), a well-known secondary phase formed during synthesis of Cu_2ZnSnS_4.[13] We could observe two structural transitions of this Cu_2S impurity phase up to ~20 GPa, in agreement with an earlier study.[42]

Upon increasing pressure, the lattice of Cu_2ZnSnS_4 shrinks anisotropically, with the *c*-axis being more compressible than *a*-axis up to ~7 GPa. Beyond that pressure, a "kink" in the pressure-induced evolution of the *c*-axis and a compressibility change of the *a*-axis is detected between 7 and 9 GPa (Figs. 4 and S5 in supplementary material). In order to identify whether this "anomaly" originates from (subtle) structural effects, we have plotted the normalized stress *F* as a function of the Eulerian strain f_E[43] (Fig. S6 in supplementary material). Generally, the F-f_E parameters should exhibit a linear correlation, with potential divergence from a linear trend implying structural changes.[44] Plotting of the F-f_E parameters reveals a break between 7 and 9 GPa, thus pointing to a structural transition of Cu_2ZnSnS_4 occurring at that pressure. Considering (a) our Raman observations, where a disordered kesterite phase was estimated to become dominant at about 9 GPa [inset in Fig. 2(a)], and (b) the fact that Cu/Zn disorder is expected to cause such "anomaly" in the *c*-axis (as observed experimentally upon increasing temperature[45]), we attribute the kink in the compression curve of the *c*-axis to a KS-to-DKS order-disorder transition taking place within the 7–9 GPa pressure range. Close examination of the unit cell volume reveals a drop of ~0.5% (as estimated by extrapolation), thus classifying the KS-to-DKS transition as of first-order. We note that the KS-to-DKS transition in our XRD study appears rather abrupt, contrary to its *gradual* character determined from our Raman study [inset in Fig. 2(a)]. A plausible reason behind this discrepancy is that, the XRD study is not able to clearly differentiate between the KS and DKS phases, since the latter results from the KS structure by the anti-site exchange of the isoelectronic Cu^+ and Zn^{2+} cations (Fig. 1), which in turn hinders the detailed monitoring of the KS-to-DKS transition in our XRD investigation.

Further compression leads to another structural transition towards a rocksalt-type (RS) structure at ~15 GPa (Figs. 3 and S4 in supplementary material), in excellent agreement with our Raman observations [Fig. 2(b)]. The DKS-to-RS transition is accompanied by a ~13% volume drop at the transition point [Fig. 4(b)], due to the coordination increase of the metal cations with respect to sulfur anions from fourfold to sixfold. Given that the kesterite phase is structurally related to the sphalerite- and chalcopyrite-type structures,[10] the pressure-induced transition towards a RS-type phase is

consistent with the general trend of the latter structures upon compression.[46,47] As for the observation of Raman signal in the stability range of the Raman-inactive NaCl-type phase [inset in Fig. 2(b)], we should bear in mind that the RS-type phase in our case is composed of different metal cations sitting at the Na site, which may lead to disorder-induced scattering.[48] Finally, we mention that this two-stage pressure-induced disorder process, i.e., from ordered to disordered kesterite, and then to disordered rocksalt-type resembles the behavior of several defect chalcopyrites under pressure.[49,50]

Turning to the equation of state (EoS) for all of the observed Cu_2ZnSnS_4 phases, we have fitted the extracted *P-V* data with third-order (KS) and second-order (DKS and RS) Birch-Murnaghan EoS functions[51] [Fig. 4(b)]. The respective results are summarized in Table S1 of the supplementary material. The most interesting observation is the large value of the KS bulk modulus derivative $B'_0 = 14.4(4)$. Attempts to fit the KS *P-V* data fixing the value of B'_0 between 4 and 8, a common range for various classes of materials,[52] resulted in poor fits (Fig. S5 in supplementary material). This large B'_0 value stems from the anisotropic compressibility of the KS phase, which most likely leads to the increased repulsion between neighboring ions (for more details, see Refs. 53 and 54). Such high B'_0 values appear to be the norm for layered systems.[44,55]

Regarding now, the mechanism of the observed pressure-induced structural transitions, it is clear that the KS-to-DKS transition results from the anti-site occupancy of the Zn and Cu cations located at the $z = 1/4$ and $z = 3/4$ layers (Fig. 1). As we mentioned already, this type of disorder has a relatively low formation energy,[11,12] thus making it favorable even under moderate perturbations.[21] On the other hand, the transition towards the RS-type phase is most likely triggered by steric effects, i.e., the tendency of materials towards higher cationic coordinations upon compression. Since these transitions can be accompanied by significant electronic changes such as insulator-to-metal transitions,[56] we have additionally performed infrared (IR) reflectance investigations for exploring this scenario; our preliminary experiments, however, did not provide a conclusive answer (Fig. S7 in supplementary material). Future experiments are scheduled to clarify this issue.

In conclusion, we have investigated the high-pressure structural and vibrational behavior of the ordered Cu_2ZnSnS_4 compound. Our investigations revealed two pressure-induced structural transitions: a kesterite-to-disordered kesterite transition taking place between 7 and 9 GPa, which involves Zn/Cu cationic disorder, whereas a rocksalt-type structure was produced at ~15 GPa. The predicted pressure-induced kesterite-to-stannite transition[17] was not detected in our investigation. Since the difference between the KS and ST structures arises from a different type of cationic ordering,[18] i.e., the cations retain their tetrahedral coordination, the adoption of the RS-type structure at ~15 GPa with sixfold cationic coordination excludes the stannite phase as a high-pressure Cu_2ZnSnS_4 polymorph at room temperature. Furthermore, our high-pressure Raman study has additionally shown that the aforementioned Zn/Cu cationic disorder will *always* be present in Cu_2ZnSnS_4 under moderate compression. This may be the reason why a full cationic order has been observed exclusively in kesterite powders and not in thin films, a particularly important result for Cu_2ZnSnS_4 thin film applications where the size mismatch between the film and its underlying substrate may result in compressive strains.

See supplementary material for additional Raman- and XRD-related data, the F-f_E plots, and the high-pressure IR reflectance spectra.

Parts of this research were carried out at the light source PETRA III (DESY), a member of the Helmholtz Association (HGF). Financial support from the MatSEC graduate school of the Helmholtz Zentrum Berlin (HZB) in cooperation with the Dahlem Research School is gratefully acknowledged (A.R.).

[1]H. Katagiri, K. Jimbo, W. S. Maw, K. Oishi, M. Yamazaki, H. Araki, and A. Takeuchi, Thin Solid Films **517**, 2455 (2009).
[2]X. Liu, Y. Feng, H. Cui, F. Liu, X. Hao, G. Conibeer, D. B. Mitzi, and M. Green, Prog. Photovoltaics **24**, 879 (2016).
[3]J. J. Scragg, P. J. Dale, L. M. Peter, G. Zoppi, and I. Forbes, Phys. Status Solidi **245**, 1772 (2008).
[4]S. Siebentritt and S. Schorr, Prog. Photovoltaics **20**, 512 (2012).
[5]S. Chen, X. G. Gong, A. Walsh, and S.-H. Wei, Appl. Phys. Lett. **94**, 41903 (2009).
[6]K. Sun, C. Yan, F. Liu, J. Huang, F. Zhou, J. A. Stride, M. Green, and X. Hao, Adv. Energy Mater. **6**, 1600046 (2016).
[7]W. Shockley and H. J. Queisser, J. Appl. Phys. **32**, 510 (1961).
[8]L. Choubrac, M. Paris, A. Lafond, C. Guillot-Deudon, X. Rocquefelte, and S. Jobic, Phys. Chem. Chem. Phys. **15**, 10722 (2013).
[9]S. Schorr, Sol. Energy Mater. Sol. Cells **95**, 1482 (2011).
[10]S. Schorr, Thin Solid Films **515**, 5985 (2007).
[11]S. Chen, X. G. Gong, A. Walsh, and S. H. Wei, Appl. Phys. Lett. **96**, 21902 (2010).
[12]S. Chen, J.-H. Yang, X. G. Gong, A. Walsh, and S.-H. Wei, Phys. Rev. B **81**, 245204 (2010).
[13]L. E. V. Rios, K. Neldner, G. Gurieva, and S. Schorr, J. Alloys Compd. **657**, 408 (2016).
[14]R. Caballero, E. Garcia-Llamas, J. M. Merino, M. Leon, I. Babichuk, V. Dzhagan, V. Strelchuk, and M. Valakh, Acta Mater. **65**, 412 (2014).
[15]M. Grossberg, J. Krustok, J. Raudoja, and T. Raadik, Appl. Phys. Lett. **101**, 102102 (2012).
[16]C.-R. Li, Y.-F. Li, B. Yao, G. Yang, Z.-H. Ding, R. Deng, and L. Liu, Phys. Lett. A **377**, 2398 (2013).
[17]Y. Zhao, D. Li, and Z. Liu, Mod. Phys. Lett. B **30**, 1650176 (2016).
[18]The stannite phase (SG $I\bar{4}2m$, $Z = 2$) exhibits a different type of cation ordering, with alternating layers of Zn/Sn and Cu along *c*-axis.
[19]P. A. Fernandes, P. M. P. Salome, and A. F. da Cunha, J. Alloys Compd. **509**, 7600 (2011).
[20]X. Fontane, V. Izquierdo-Roca, E. Saucedo, S. Schorr, V. O. Yukhymchuk, M. Y. Valakh, A. Perez-Rodriguez, and J. R. Morante, J. Alloys Compd. **539**, 190 (2012).
[21]J. J. S. Scragg, L. Choubrac, A. Lafond, T. Ericson, and C. Platzer-Bjorkman, Appl. Phys. Lett. **104**, 41911 (2014).
[22]M. Y. Valakh, V. M. Dzhagan, I. S. Babichuk, X. Fontane, A. Perez-Rodriquez, and S. Schorr, JETP Lett. **98**, 255 (2013).
[23]A. Ritscher, J. Just, O. Dolotko, S. Schorr, and M. Lerch, J. Alloys Compd. **670**, 289 (2016).
[24]H. K. Mao, J. Xu, and P. Bell, J. Geophys. Res. **91**, 4673, doi:10.1029/JB091iB05p04673 (1986).
[25]H.-P. Liermann, Z. Konopkova, W. Morgenroth, K. Glazyrin, J. Bednarcik, E. E. McBride, S. Petitgirard, J. T. Delitz, M. Wendt, Y. Bican, A. Ehnes, I. Schwark, A. Rothkirch, M. Tischer, J. Heuer, H. Schulte-Schrepping, T. Kracht, and H. Franz, J. Synchrotron Radiat. **22**, 908 (2015).
[26]A. P. Hammersley, S. O. Svensson, M. Hanfland, A. N. Fitch, and D. Hausermann, High Pressure Res. **14**, 235 (1996).
[27]B. H. Toby, J. Appl. Crystallogr. **34**, 210 (2001).
[28]A. Ritscher, M. Hoelzel, and M. Lerch, J. Solid State Chem. **238**, 68 (2016).
[29]S. Klotz, J.-C. Chervin, P. Munsch, and G. Le Marchand, J. Phys. D: Appl. Phys. **42**, 75413 (2009).

[30]D. Errandonea, R. Boehler, S. Japel, M. Mezouar, and L. R. Benedetti, Phys. Rev. B **73**, 92106 (2006).
[31]M. Ross, H. K. Mao, P. M. Bell, and J. A. Xu, J. Chem. Phys. **85**, 1028 (1986).
[32]J. Wittlinger, R. Fischer, S. Werner, J. Schneider, and H. Schulz, Acta Crystallogr. B **53**, 745 (1997).
[33]M. Koch-Müller, S. Speziale, F. Deon, M. Mrosko, and U. Schade, Phys. Chem. Miner. **38**, 65 (2011).
[34]A. Khare, B. Himmetoglu, M. Johnson, D. J. Norris, M. Cococcioni, and E. S. Aydil, J. Appl. Phys. **111**, 83707 (2012).
[35]M. Dimitrievska, A. Fairbrother, X. Fontane, T. Jawhari, V. Izquierdo-Roca, E. Saucedo, and A. Perez-Rodriguez, Appl. Phys. Lett. **104**, 21901 (2014).
[36]M. Dimitrievska, A. Fairbrother, A. Perez-Rodriguez, E. Saucedo, and V. Izquierdo-Roca, Acta Mater. **70**, 272 (2014).
[37]O. Gomis, R. Vilaplana, F. J. Manjon, E. Perez-Gonzalez, J. Lopez-Solano, P. Rodriguez-Hernandez, A. Munoz, D. Errandonea, J. Ruiz-Fuertes, A. Segura, D. Santamaria-Perez, I. M. Tiginyanu, and V. V. Ursaki, J. Appl. Phys. **111**, 13518 (2012).
[38]O. Gomis, R. Vilaplana, F. J. Manjon, D. Santamaria-Perez, D. Errandonea, E. Perez-Gonzalez, J. Lopez-Solano, P. Rodriguez-Hernandez, A. Munoz, I. M. Tiginyanu, and V. V. Ursaki, Mater. Res. Bull. **48**, 2128 (2013).
[39]D. Errandonea, R. S. Kumar, O. Gomis, F. J. Manjon, V. V. Ursaki, and I. M. Tiginyanu, J. Appl. Phys. **114**, 233507 (2013).
[40]O. Gomis, D. Santamaria-Perez, R. Vilaplana, R. Luna, J. A. Sans, F. J. Manjon, D. Errandonea, E. Perez-Gonzalez, P. Rodriguez-Hernandez, A. Munoz, I. M. Tiginyanu, and V. V. Ursaki, J. Alloys Compd. **583**, 70 (2014).
[41]D. Santamaria-Perez, M. Amboage, F. J. Manjon, D. Errandonea, A. Munoz, P. Rodriguez-Hernandez, A. Mujica, S. Radescu, V. V. Ursaki, and I. M. Tiginyanu, J. Phys. Chem. C **116**, 14078 (2012).
[42]D. Santamaria-Perez, G. Garbarino, R. Chulia-Jordan, M. A. Dobrowolski, C. Muehle, and M. Jansen, J. Alloys Compd. **610**, 645 (2014).
[43]R. J. Angel, Rev. Mineral. Geochem. **41**, 35 (2000).
[44]A. Polian, M. Gauthier, S. M. Souza, D. M. Triches, J. C. de Lima, and T. A. Grandi, Phys. Rev. B **83**, 113106 (2011).
[45]S. Schorr and G. Gonzalez-Aviles, Phys. Status Solidi A **206**, 1054 (2009).
[46]M. S. Miao and W. R. L. Lambrecht, Phys. Rev. Lett. **94**, 225501 (2005).
[47]R. S. Kumar, A. Sekar, N. V. Jaya, S. Natarajan, and S. Chichibu, J. Alloys Compd. **312**, 4 (2000).
[48]J. Ibanez, R. Oliva, F. J. Manjon, A. Segura, T. Yamaguchi, Y. Nanishi, R. Cusco, and L. Artus, Phys. Rev. B **88**, 115202 (2013).
[49]V. V. Ursaki, I. I. Burlakov, I. M. Tiginyanu, Y. S. Raptis, E. Anastassakis, and A. Anneda, Phys. Rev. B **59**, 257 (1999).
[50]F. J. Manjon and R. I. Vilaplana, *Pressure-Induced Phase Transitions in AB_2X_4 Chalcogenide Compounds* (Springer-Verlag, Berlin, Heidelberg, 2014).
[51]F. Birch, Phys. Rev. **71**, 809 (1947).
[52]A. M. Hofmeister, Geophys. Res. Lett. **20**, 635, doi:10.1029/93GL00388 (1993).
[53]I. V. Aleksandrov, A. F. Goncharov, A. N. Zisman, and S. M. Stishov, J. Exp. Theor. Phys. **66**, 384 (1987).
[54]E. Stavrou, M. R. Manaa, J. M. Zaug, I.-F. W. Kuo, P. F. Pagoria, B. Kalkan, J. C. Crowhurst, and M. R. Armstrong, J. Chem. Phys. **143**, 144506 (2015).
[55]M. O. Filso, E. Eikeland, J. Zhang, S. R. Madsen, and B. B. Iversen, Dalton Trans. **45**, 3798 (2016).
[56]A. Mujica, A. Rubio, A. Munoz, and R. J. Needs, Rev. Mod. Phys. **75**, 863 (2003).